Supporting Information

Edie et al. 10.1073/pnas.1717636115

Datasets

Recent Marine Bivalve Dataset. Extant species and genus range limits are available from the supplement to ref. 1. The dataset includes 60,942 occurrence records of 5,903 species in 1,073 genera at water depths <200 m compiled from the literature and museum collections (1). Functional assignments are in the supplement to ref. 2.

Era Boundaries Marine Bivalve Dataset. We compiled from the literature and taxonomically/stratigraphically standardized a global record of marine bivalves occurring in the Guadalupian stage of the Permian and the Maastrichtian stage of the Cretaceous (Dataset S1). Survival of FGs through the PT and KPg was marked by the occurrence of a preextinction genus in Triassic or later strata for the PT and Danian or later strata for the KPg. In cases where no genera within an FG have been sampled after the extinction, we assumed the FGs survived the event if the families of those genera were monofunctional and sampled in later stratigraphic intervals; i.e., we allowed for phylogenetic continuity across the extinction.

We collected the largest reported body size (geometric mean of shell length and height in millimeters) (3) of individuals within Guadalupian and Maastrichtian genera using the literature. When we were unable to recover a size from an individual in those intervals, we used the body size of stratigraphically lower individuals within the Permian and the Cretaceous, respectively. Inclusion or exclusion of these body sizes from outside the target time periods does not change the body size patterns in Fig. 2*B* (Dataset S1).

Analytical Code Dataset. Dataset S2 contains R code necessary for reproducing figures and values referenced in this paper, as well as the simulations described in *FR and FE Through the Mass Extinctions*.

FR and FE Through the Mass Extinctions

Ideally, we would compare the FE of the preextinction fauna directly to the FE of the fauna that survived the mass extinctions (the PT and the KPg). However, notably poor preservation of the earliest Triassic bivalve fauna (4–6) and of the earliest Paleogene fauna (7) hinders a robust assessment of the change in FE across the extinction events. Thus, we examined expected changes in the number of FGs and in FE under the two extinction scenarios described below.

Scenario 1: Stochastic Extinction. We used the estimated extinction intensity of marine bivalve genera across each boundary to simulate random extinction of genera across all FGs. For example, our genus-level extinction intensity across the PT was 76% (127 genera went extinct of 167 total), leaving a minimum of 40 surviving genera. Therefore, we randomly sampled 40 genera from the preextinction fauna (the 167 Guadalupian genera) and repeated the simulation 1,000 times to generate a distribution of possible surviving faunal sets. We summarized the number of surviving FGs across each simulation to recover a distribution of expected FGs given the distribution of taxa within the Guadalupian faunal set. We repeated this simulation across additional extinction intensities ranging from 0% to 100% of genera to determine plausible levels of stochastic extinction that would generate the survival of all or nearly all FGs.

The observed extinction intensity (76% across the PT and 64% across the KPg) is necessarily a high-end estimate as we assume only one genus within Lazarus families survives. We also considered a possible low-end estimate of extinction, where we constrained all genera belonging to Lazarus families in the preextinction fauna to survive. Sampling may improve the record of surviving genera within non-Lazarus families as well and could further lower extinction estimates (assuming that the discovery of new, surviving, non-Lazarus genera outpaces the discovery of new genera that went extinct), but rarity, low taxonomic richness, and/or poor preservation are more commonly correlated with Lazarus families (5). Under this low-end estimate of extinction intensity, the proportion of genera lost decreases to 64% across the PT and 56% across the KPg.

Scenario 2: Stochastic Extinction with Survival of Functional Groups. Empirically, all or nearly all of the FGs survive both the PT and the KPg. Thus, the purely stochastic extinction scenario above may not accurately reflect the style of extinction observed in the fossil record. Because of the aforementioned sampling issues in the postextinction faunas, we simulated the survival of taxa to estimate a range of likely FE values under random extinction with the constraint of observed FG survival. First, we constrained the survival of FGs by allowing 1 genus from each FG of the preextinction fauna to survive. In the Permian dataset, that equates to 17 genera surviving from the Guadalupian fauna, 1 from each FG known to have survived the extinction. We then randomly sampled the remaining survivors (23 survivor spots open in the Permian survival pool because 76% extinction of 167 genera = 40 survivors – 17 surviving FGs = 23 surviving genera) from the now depleted preextinction pool (150 genera remain in the Guadalupian fauna). In this simulation, FGs cannot acquire more taxa than were present in the preextinction fauna. We estimated the FE of each simulated surviving fauna (1,000 simulations) and then summarized FE values across simulations (e.g., Fig. S2*C*). This semistochastic extinction scenario provides an expectation for whether the FE of the surviving fauna could have increased above that of the preextinction fauna.

Permian–Triassic Extinction. All or all but one of the 17 FGs present in the Guadalupian bivalve fauna survived the end-Permian (Fig. 2*A*). Under stochastic taxonomic extinction at the observed intensity of 76% (scenario 1 described above), only 11 of 17 Guadalupian FGs are expected to survive, and no simulated extinctions demonstrate the survival of all 17 FGs (Fig. S2*B*). Under the lower-end extinction intensity of 64%, only 13 FGs are expected to survive and no simulated extinctions result in the survival of all 17 FGs. Consistent recovery of all 17 FGs appears to require extinction intensities below 30%, which is well below our low-end extinction estimate and estimates made in other studies (8, 9). Thus, the extinction pattern of FGs through stochastic extinction is inconsistent with the observed extinction pattern, suggesting the observed extinction selectivity may have led to an asymmetric loss of genera from taxonomically rich FGs and persistence of genera from taxonomically depauperate FGs (see survivorship patterns discussed in *Asymmetric Functional Selectivity* in the main text).

Results from the simulations above suggest that FE must have increased across the PT because the low-richness FGs persisted, therefore requiring high-richness FGs to have suffered relatively heavier losses. However, depending on the extinction intensity, the evenness of the surviving fauna may have decreased if the low-richness FGs sustained relatively more extinctions than the high-richness FGs. This scenario of lowered evenness approaches

a mathematical impossibility under the constraint of survival of all FGs and the extinction intensity increases above the observed value (scenario 2 above), but lower extinction intensities may lead to FE values lower than the observed value in the Guadalupian (0.38, Fig. S2*A*). Under the observed extinction intensity of 76% where all FGs are constrained to survive, the simulated extinctions increased the FE of the surviving fauna to 0.54 (Fig. S2*C*) and only 0.2% of simulations resulted in a lower FE. The low-end extinction intensity of 64% also increased FE over the observed value (Fig. S2*C*). Only when simulated extinction intensities fall below 50% does the frequency of surviving faunas with lower FE than the observed value rise above 10%, becoming a possible extinction outcome. However, 50% is again far below the previously recorded extinction intensities through this event (8, 9). Thus, the infrequency of simulations with surviving faunas of higher FE than observed in the Guadalupian suggests that the end-Permian extinction is likely to have increased FE, asymmetrically selecting against the survival of genera within high-richness FGs and for the survival of genera within low-richness FGs.

Cretaceous–Paleogene Extinction. Only 2 of 30 FGs did not survive the end-Cretaceous extinction (Fig. 2*B*). At the observed extinction intensity of 64%, 24 FGs are expected to survive across simulations and 27 or more FGs survive in only 1.5% of simulated extinctions (Fig. S2*E*). Under the low-end extinction intensity of 56%, 25 FGs are expected to have survived and the frequency of simulations with at least 28 surviving FGs remains relatively low at 8%.

Across the KPg, 2 of 30 FGs possibly go extinct, differing from the survival of possibly all FGs across the PT. Unlike the PT, the scenario that the extinction decreased the evenness of the surviving fauna becomes more probable if the extinction is concentrated within those extinct FGs—a real possibility for the Maastrichtian fauna given the strong selection against the rudist bivalves (5). Before the extinction, the observed FE of the Maastrichtian fauna is 0.39 (Fig. S2*C*). An extinction intensity of 64% under the conditions described in scenario 2 above would have likely increased the evenness of the surviving fauna (FE of 0.44 with 94% of simulations resulting in a higher FE than the observed 0.39; Fig. S2*F*). The low-end extinction intensity of 56% also increased the expected FE of the surviving fauna to 0.42 and 90% of simulations increased the FE of the surviving fauna. The simulated FE values from the observed to the low-end extinction intensities suggest that stochastic extinction would have likely resulted in a more even distribution of taxa among FGs similar to the end-Permian extinction.

1. Tomašových A, et al. (2016) Unifying latitudinal gradients in range size and richness across marine and terrestrial systems. *Proc R Soc B* 283:20153027.
2. Berke SK, Jablonski D, Krug AZ, Valentine JW (2014) Origination and immigration drive latitudinal gradients in marine functional diversity. *PLoS One* 9: e101494.
3. Kosnik M, Jablonski D, Lockwood R, Novack-Gottshall P (2006) Quantifying molluscan body size in evolutionary and ecological analyses: Maximizing the return on data-collection efforts. *Palaios* 21:588–597.
4. Erwin DH (2006) *Extinction: How Life on Earth Nearly Ended 250 Million Years Ago* (Princeton Univ Press, Princeton).
5. Jablonski D (1986) Causes and consequences of mass extinctions: A comparative approach. *Dynamics of Extinction*, ed. Elliott DK (Wiley, New York), pp 183–229.
6. Fraiser ML, Clapham ME, Bottjer DJ (2011) Mass extinctions and changing taphonomic processes fidelity of the Guadalupian, Lopingian, and early Triassic fossil records. *Taphonomy: Process and Bias Through Time*, eds Allison PA, Bottjer DJ (Springer, Berlin), Vol 32, 2nd Ed, pp 569–590.
7. Sessa JA, Patzkowsky ME, Bralower TJ (2009) The impact of lithification on the diversity, size distribution, & recovery dynamics of marine invertebrate assemblages. *Geology* 37:115–118.
8. Tu C, Chen ZQ, Harper DAT (2016) Permian-Triassic evolution of the Bivalvia: Extinction-recovery patterns linked to ecologic and taxonomic selectivity. *Palaeogeogr Palaeoclimatol Palaeoecol* 459:53–62.
9. Stanley SM (2016) Estimates of the magnitudes of major marine mass extinctions in Earth history. *Proc Natl Acad Sci USA* 113:E6325–E6334.

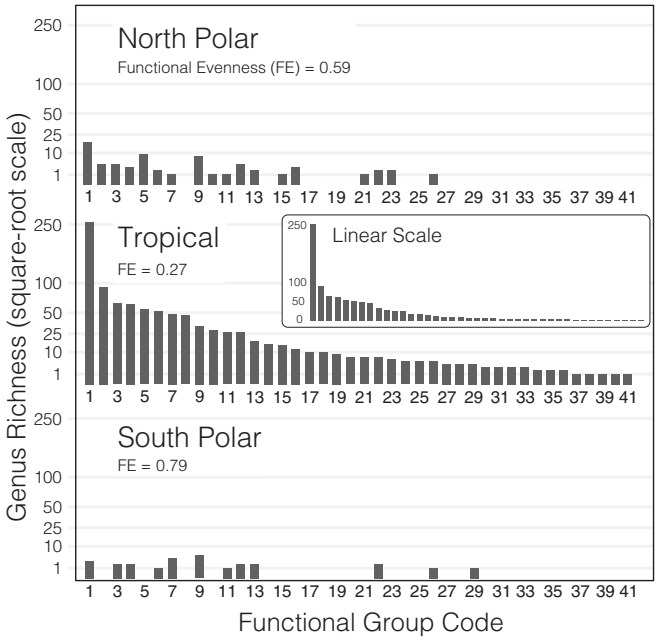

Fig. S1. Taxonomic richness (genus level) of marine bivalve functional groups within the modern tropics and poles. The distribution of tropical genera within functional groups follows a characteristic "hollow" curve, with most genera occurring in the richest functional groups. Functional group codes are defined in Table S1.

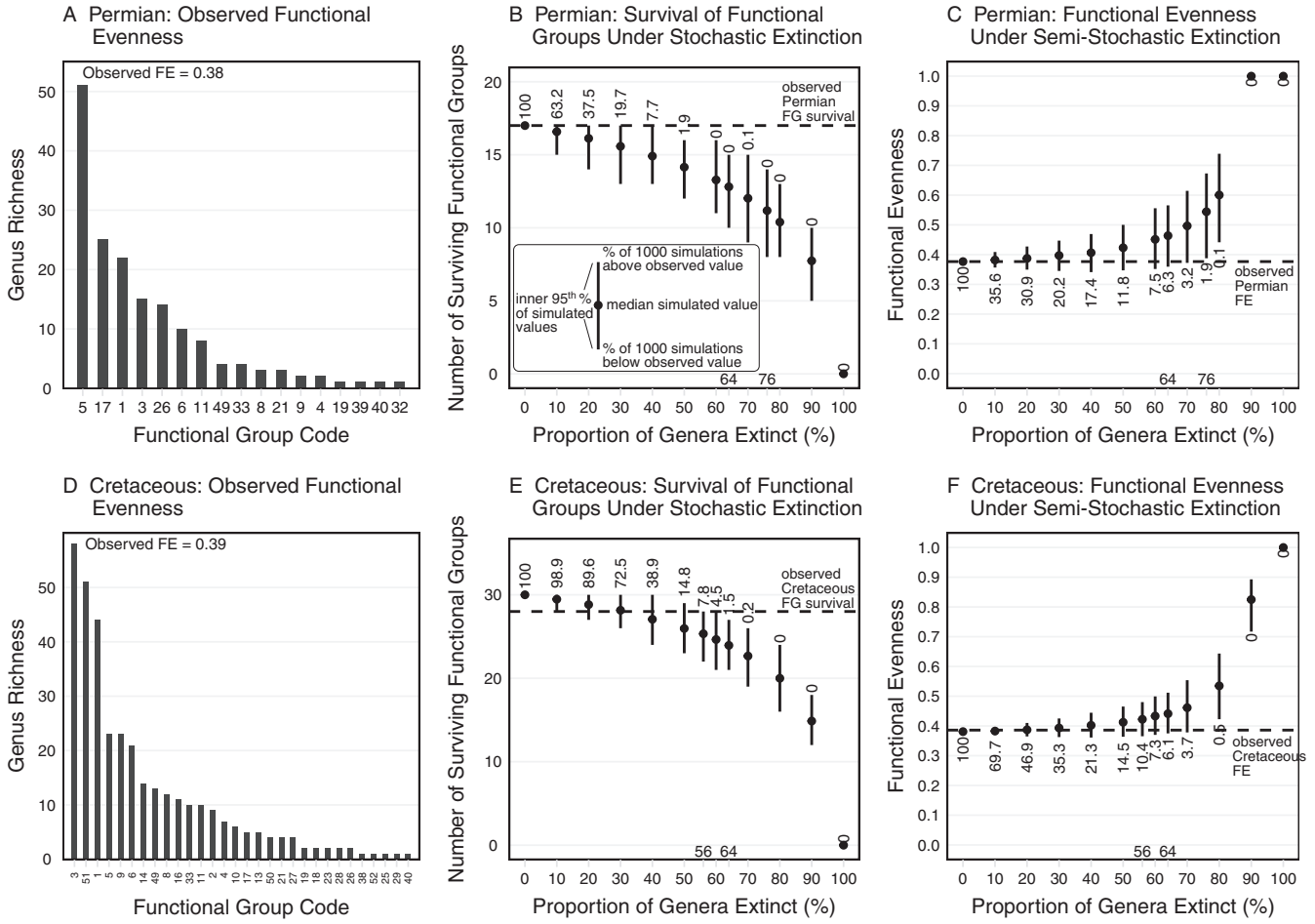

Fig. S2. (*A*) The observed distribution of Permian (Guadalupian) genera within FGs. FG codes are defined in Table S1. (*B*) The simulated survival of FGs across the PT through stochastic taxonomic extinction. With increasing taxonomic extinction intensity (i.e., goes to 100%), the simulated number of surviving FGs drops to 0. For the observed extinction intensity of the Guadalupian fauna (76%), only 11 of the 17 FGs are expected to survive, and only 0 of the 1,000 simulated extinctions exhibits the survival of all 17 FGs. (*C*) The simulated changes in FE of the surviving Guadalupian fauna under stochastic extinction where all FGs are constrained to survive (i.e., at least one genus from each FG survives the extinction). As the intensity of taxonomic extinction increases, the expected evenness of genera among FGs increases toward the maximum evenness (value of 1). For the observed extinction intensity of the Guadalupian fauna (76%), the simulated evenness of 0.54 is much higher than the observed initial evenness of 0.38, and only 1.9% of the 1,000 simulations exhibit an evenness equal to or lower than the observed value. (*D*) The observed distribution of Cretaceous (Maastrichtian) genera within FGs. (*E*) The simulated survival of FGs across the KPg through stochastic taxonomic extinction. Similar to the end-Permian in *B*, the simulated number of surviving FGs drops to 0 as the intensity of taxonomic extinction increases. For the observed extinction intensity of the Maastrichtian fauna (64%), only 24 of the 30 FGs are expected to survive, and only 1.5% of the 1,000 simulated extinctions exhibit the survival of all 28 FGs known to survive the extinction. (*F*) The simulated changes in functional evenness of the surviving Maastrichtian fauna under stochastic extinction where the 28 of 30 FGs known to survive are constrained to survive. Similar to the simulations for the Permian in *C*, the simulated evenness of genera among FGs increases toward the maximum evenness (value of 1) as the intensity of taxonomic extinction increases. For the observed extinction intensity of the Maastrichtian fauna (64%), the simulated evenness of 0.44 is higher than the observed initial evenness of 0.39, and only 6.1% of the 1,000 simulations exhibit an evenness equal to or lower than the observed value.

Table S1. Definitions of FG codes used in figures

FG	Mobility	Substrate	Feeding	Fixation
1	Mobile	Shallow infaunal siphonate	Suspension	Unattached
2	Mobile	Shallow/deep infaunal siphonate	Mixed deposit/suspension	Unattached
3	Mobile	Infaunal asiphonate	Suspension	Unattached
4	Mobile	Deep infaunal siphonate	Chemosymbiotic	Unattached
5	Immobile	Epifaunal	Suspension	Byssate
6	Mobile	Deep infaunal siphonate	Suspension	Unattached
7	Mobile	Shallow infaunal siphonate	Suspension	Byssate
8	Mobile	Epifaunal	Suspension	Byssate
9	Immobile	Epifaunal	Suspension	Cemented
10	Immobile	Borer	Suspension	Unattached
11	Mobile	Shallow infaunal siphonate	Subsurface deposit	Unattached
12	Mobile	Commensal	Suspension	Byssate
13	Mobile	Shallow infaunal siphonate	Carnivore	Unattached
14	Swimming	Epifaunal	Suspension	Byssate
15	Mobile	Shallow infaunal siphonate	Surface deposit	Unattached
16	Immobile	Shallow infaunal siphonate	Suspension	Byssate
17	Immobile	Semiinfaunal	Suspension	Byssate
18	Immobile	Deep infaunal siphonate	Suspension	Unattached
19	Immobile	Borer	Suspension	Byssate
20	Mobile	Borer	Suspension	Unattached
21	Mobile	Infaunal asiphonate	Subsurface deposit	Unattached
22	Immobile	Infaunal asiphonate	Suspension	Byssate
23	Immobile	Nestler	Suspension	Byssate
24	Mobile	Deep infaunal siphonate	Surface deposit	Unattached
25	Mobile	Epifaunal	Carnivore	Byssate
26	Mobile	Semiinfaunal	Suspension	Byssate
27	Mobile	Shallow infaunal siphonate	Chemosymbiotic	Unattached
28	Mobile	Infaunal asiphonate	Suspension	Byssate
29	Mobile	Nestler	Suspension	Byssate
30	Mobile	Semiinfaunal	Suspension	Unattached
31	Mobile	Epifaunal	Suspension	Unattached
32	Swimming	Epifaunal	Suspension	Unattached
33	Immobile	Epifaunal	Suspension	Unattached
34	Mobile	Commensal	Suspension	Unattached
35	Mobile	Deep infaunal siphonate	Subsurface deposit	Unattached
36	Mobile	Semiinfaunal	Photosymbiotic	Unattached
37	Immobile	Epifaunal	Photosymbiotic	Byssate
38	Immobile	Nestler	Suspension	Unattached
39	Mobile	Infaunal asiphonate	Chemosymbiotic	Unattached
40	Swimming	Deep infaunal siphonate	Chemosymbiotic	Unattached
41	Immobile	Borer	Suspension	Cemented
42	Mobile	Deep infaunal siphonate	Carnivore	Unattached
43	Mobile	Nestler	Surface deposit	Unattached
44	Mobile	Nestler	Suspension	Unattached
45	Swimming	Deep infaunal siphonate	Suspension	Unattached
46	Swimming	Epifaunal	Carnivore	Byssate
47	Swimming	Nestler	Suspension	Byssate
48	Swimming	Semiinfaunal	Suspension	Unattached
49	Immobile	Epifaunal	Photosymbiotic?	Unattached
50	Immobile	Epifaunal	Photosymbiotic?	Cemented
51	Immobile	Semiinfaunal	Photosymbiotic?	Unattached
52	Immobile	Shallow infaunal siphonate	Suspension	Unattached

Other Supporting Information Files

Dataset S1 (XLSX)

Dataset S2 (TXT)